JOURNAL OF APPLIED POLYMER SCIENCE VOL. 18, PP. 2165–2176 (1974)

Dynamic Mechanical Behavior of Highly Filled Polymers: Energy Balances and Damage

A. H. LEPIE and A. ADICOFF, *Code 6058, Naval Weapons Center, China Lake, California 93555*

Synopsis

Dynamic tests using the Naval Weapons Center torsion–tension tester and end-bonded cylindrical propellant specimen were carried out to evaluate the effects of internal damage on propellants by subjecting samples to small tensile oscillations during low constant-strain rate tests. It is shown that microstructural damage in a propellant causes significant changes in mechanical properties. The mechanical property curves demonstrate that the response is markedly strain sensitive. So long as the maximum strain experienced by the sample during a test is not exceeded, the response of the propellant to small tensile oscillation during repeated strains below that maximum value remains relatively unchanged after the first initial dramatic change. The differences between mechanical energy balances of "undamaged" and "damaged" propellant samples were used to demonstrate microstructural damage and to estimate the extent of damage. For any one propellant, the total lost energy caused by microscopic failure of the propellant seems to be additive, constant, and independent of the mechanical path to failure.

INTRODUCTION

This paper reports on the dynamic mechanical properties of a solid propellant. A solid propellant is a conglomerate of solid particles embedded in an elastomeric binder. The application of a load to a propellant sample causes irreversible microstructural damage as a result of molecular chain scission and interfacial debonding (dewetting). A repeated test on the same sample, therefore, produces a response which differs from the preceding one. This cumulative damage behavior is a characteristic of a solid propellant.

Linear cumulative damage analysis was developed to predict formation of cracks in rocket motor grains while they are subjected to various loading conditions and to temperature cycling. The most extensive work in this area has been done by Bills,[1] Farris,[2] and other investigators.[3,4,5] In much of this work, a linear form of Miner's law is used to assess the damage done to the microstructure of a propellant. The damage is assumed to accumulate until a maximum macroscopic failure value is reached.

The original cumulative damage criterion relates the damage fraction (ΔD) in the specimen to a time increment (Δt_i) for the ith stress level and the ith time to failure (t_{fi}) under a given loading history:[1]

$$\Delta D = \Delta t_i / t_{fi}. \tag{1}$$

The cumulative damage theory requires that $\Delta D = 1.0$ when failure occurs.

These relationships can be formulated in terms of stress. Bills[1] and Farris[2] have made extensive use of the stress law and relate the time to failure ($\bar{t}_f$) of a specimen under a constant true stress (σ_t) to a critical true stress (σ_{cr}) below which no failures are observed. This paper tends to show that a strain damage criterion, rather than a stress damage criterion, governs the behavior of some propellants. If a propellant is damaged once at a certain strain level, the damage does not increase, or increases only slightly, during repeated deformation below that strain level.

The purpose of this paper is to deal less with the cumulative damage formulation itself, but to examine the phenomenologic effects of internal damage upon some mechanical properties. A nonlinear viscoelastic response in a propellant is mainly caused by complex binder–filler interactions and high local strain conditions during the sample deformation. The material is nearly linearly viscoelastic at low strains and at high strains and is definitely nonlinear viscoelastic only at moderate strains. Small oscillating deformations superposed on a finite stretch can be used to probe the nature of this material during uniaxial extension. Although the properties change as the sample is damaged, the sample shows nearly linear viscoelastic response to small superposed oscillations at early and late strains. The response to superposed torsional oscillations is more amenable to a linear viscoelastic analysis than the response to superposed tensile oscillations.

The propellant used in our composites consists of an 86 wt-% mixture of ammonium perchlorate and fine aluminum particles bound together with 14 wt-% of a hydroxyl-terminated polybutadiene cured with a diisocyanate reagent. The experiments were made in an apparatus which applies superposed sinusoidal oscillations to a specimen under finite strain.[6,7] The dynamic measurements can be made in tension and/or torsion. The apparatus is thus used essentially as a mechanical spectroscope. It is possible to calculate moduli from the nonlinear response curves obtained in this way. However, the hysteresis energies turn out to be more useful for monitoring changes in the propellant during the deformation.

THEORY

Application of finite strain to a propellant sample causes a separation between the binder and the solid particles, leading to the development of microcracks. The resulting formation of new surfaces requires a certain amount of energy which is a function of the surface area being created and of the respective cohesive and adhesive energies involved in the process.

When a propellant sample is strained at constant straining rate, the total energy input per unit volume (ΔE_t) can be determined from the area under the stress–strain curve as follows:

$$\Delta E_t = \int_{\epsilon_0}^{\epsilon_1} \sigma(\epsilon) d\epsilon. \tag{2}$$

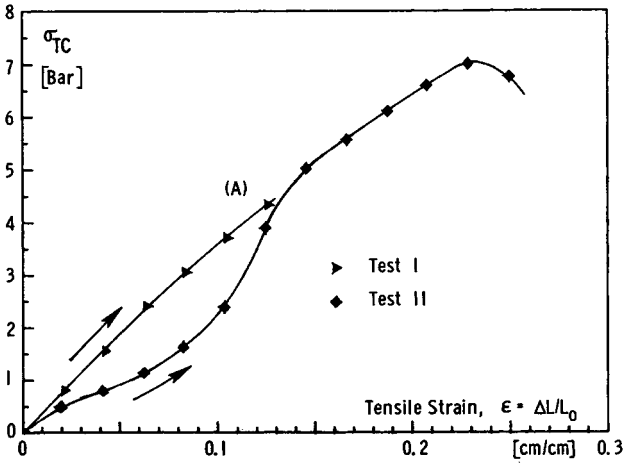

Fig. 1. Repeated uniaxial stress–strain test of a propellant.

The total input energy (ΔE_t) during deformation is the sum of an elastic part (ΔE_e) and a loss part (ΔE_l). Thus, one may write

$$\Delta E_t = \Delta E_e + \Delta E_l. \tag{3}$$

Although partitioning of the energies in this way is probably not exact, it will serve as a useful first approximation.

Figure 1 shows a typical stress–strain curve obtained on a propellant in repeated stretching. The upper curve (test I) describes the behavior of the sample on the first stretch, and the lower curve (test II) describes the second stretch after a 1-hr recovery period. On succeeding stretches, the lower curve is followed as long as the maximum strain in the first stretch (point A) is not exceeded. As many as nine successive stretches have been performed below the maximum strain of the first stretch, and no observable change in the lower curve was detected. It is therefore assumed that the area under the lower curve represents the recoverable or elastic work ΔE_e, while the difference in the area between the two curves represents the energy losses attributable to propellant damage ΔE_l. Since the dewetting effect is of the order of 10^{-3} cal/cm^3 and the effect of carbon bond rupture is of the order of 8 to 0.8 cal/cm^3 (see Appendix), it is assumed that the major contribution to the measured loss energy is the rupture of load bearing molecular chains.

The difference ΔE_ϵ in dynamic energies from superposed oscillations before and after an applied strain history, which we shall call the damage energy, is characteristic for the damage behavior of a propellant. We may write

$$\Delta E_\epsilon = \Delta E_u - \Delta E_d \tag{4}$$

where the subscript u refers to an undamaged sample and d refers to a damaged sample. The summation of the energy losses ΔE_l obtained for

successive increments in the finite stretch give characteristic curves from which the damage energy ΔE_ϵ can be determined as a function of strain. We have

$$\Delta E_\epsilon = \sum_{\epsilon_0}^{\epsilon_1} \Delta E_u - \sum_{\epsilon_0}^{\epsilon_1} \Delta E_d \tag{5}$$

where ΔE_u and ΔE_d now refer to the curves obtained with each increment. The fractional energy loss f_E between the two strains ϵ_0 and ϵ_{max} can be computed from

$$f_E = \frac{\Delta E_\epsilon}{\Delta E_{\epsilon_{max}}}. \tag{6}$$

A plot of the fractional energy losses f_E and the fractional energy losses per unit strain, f_E/ϵ, as a function of strain can be considered as qualitative indicators of the degree of linearity of the cumulative damage criterion.

SAMPLE PREPARATION AND DETERMINATION OF STRAIN

End-bonded square samples were found unsatisfactory for a failure test because rupture invariably occurred in the region of highest stress concentration near the end of the sample. In addition, corner stress anomalies made the data difficult to interpret. Samples with a cylindrical cross section were used, therefore, to obtain rupture data in regions of homogeneous uniaxial stress. A simple and inexpensive miniature lathe was developed to allow us to mill an end-bonded sample with square cross section into a cylindrical shape with contoured conical ends.

Conversion factors were used to compute the strain in the gauge section of the sample from the observed cross-head displacement. The strain-dependent conversion factor was determined from a comparison of the cross-head displacement with the displacement of bench marks observed with a traveling microscope. Photographic techniques were found to lack reliability because of depth of field and edge resolution problems.

EXPERIMENTAL PROCEDURE

The sample is placed into an Instron tester which has been modified with a dynamic tension–torsion testing device.[6,7] This modification enables the simultaneous or alternate forced vibrations in tension and torsion to be applied to the specimen over a frequency range of 0.002 Hz to 5 Hz and with adjustable amplitudes of 0 to 0.3 cm and 0 to 12 degrees, respectively. The sample is simultaneously strained at the Instron tester straining rates during the oscillations. Tensile force measurements are made with a 50-lb Photocon load cell. The standard Instron load cell was not used because an electrical phase shift was observed in the output.

The effect of internal damage on different material properties was studied by straining the sample at a constant low strain rate of 0.04 cm/min. During this test, superposed tensile oscillations with a frequency of 0.5 Hz and

an amplitude of ±0.05 cm were applied. The tensile force at the lower-amplitude was recorded separately during the straining of the sample. In addition, the force-displacement hysteresis loops were recorded on an X-Y recorder. At predetermined strain levels, the test runs were interrupted in order to obtain samples with defined amounts of microstructural damage. These samples were allowed to recover for 1 hr without application of external stress. The samples were then repeatedly strained and cycled under the following strain conditions: test A, 0 to 6%; test B, 0 to 12%; test C, 0 to 18%; and test D, 0% to failure.

EVALUATION OF MEASUREMENTS

The following characteristic values were determined at each strain level: (1) minimum tensile stress during superposed oscillation (σ_1); (2) maximum tensile stress during superposed oscillation (σ_2); (3) dynamic tensile stress ($\Delta\sigma = \sigma_2 - \sigma_1$); (4) total energy input per cycle (ΔE_t); (5) energy loss per cycle (ΔE_l); (6) recovered energy per cycle (ΔE_e); and (7) phase shift angle between the sinusoidal force input and the strain response (tan ϕ).

The nonlinear viscoelastic behavior of the propellant lead to nonelliptical hysteresis loops and makes the analysis of the behavior in terms of moduli difficult. After a few attempts to apply nonlinear viscoelastic constitutive equations to the data, the approach was discarded and the data were treated in terms of stresses, displacements, energies, and phase shifts. The hysteresis energies were computed from the areas measured with a planimeter.

RESULTS

The superposed sinusoidal tensile oscillations during straining cause an oscillating stress response with maximum and minimum values σ_2 and σ_1, respectively. Figure 2 shows the oscillating stresses during test C. The

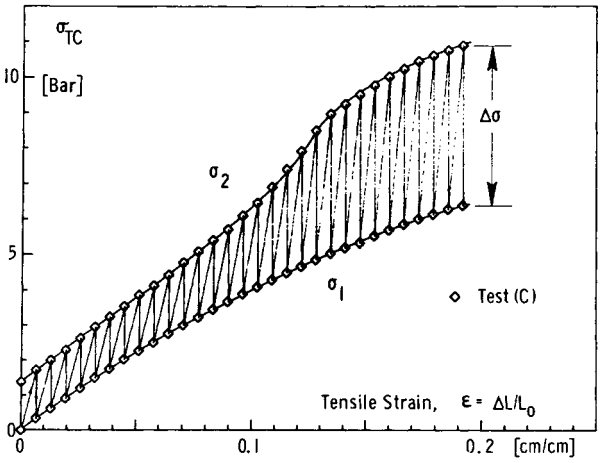

Fig. 2. Oscillating stresses during combined straining and cycling.

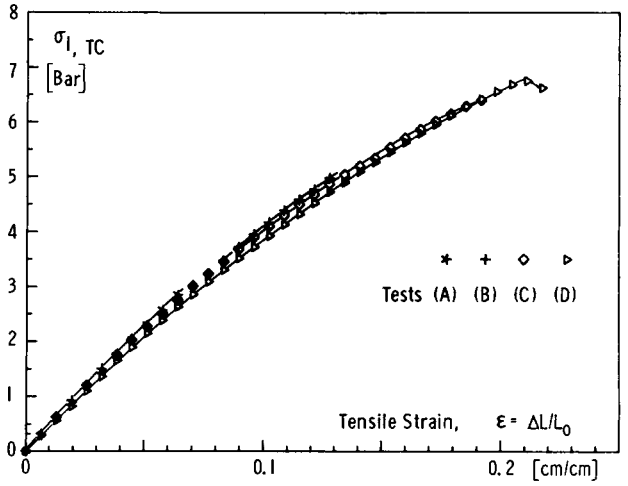

Fig. 3. Minimum cycling stresses during tests A to D.

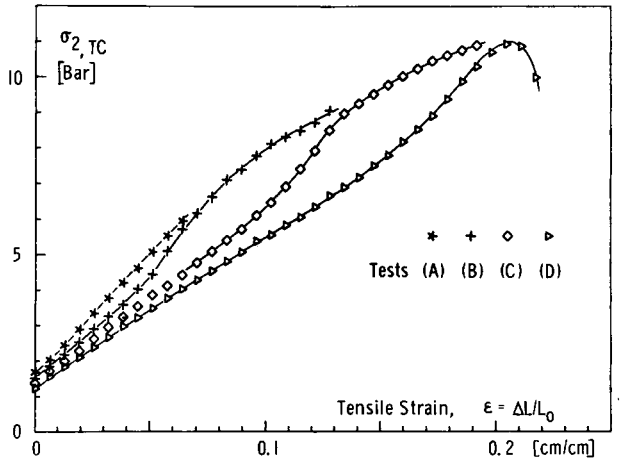

Fig. 4. Maximum cycling stresses during tests A to D.

area between the curves represents the characteristic specimen cycling energy. The stresses, σ_1 and σ_2, obtained in the repeated tests A through D are plotted in Figures 3 and 4 versus applied strain. It can be seen that the internal damage affects the minimum and maximum oscillation stresses differently. The σ_2 curves clearly show a softening of the material after each straining experiment with increasing strain, while the σ_1 curves indicate almost no effect on the minimum cycling stresses. The dynamic cycling stress $\Delta\sigma = \sigma_2 - \sigma_1$ shows a more sensitive reaction to the damage than the maximum stress σ_2, as can be seen from Figure 5. The loss tangent at zero strain was found to be the only measured property which increased with increasing amounts of damage. Figure 6 shows that the initial values of tan ϕ near zero strain are slightly increased from test

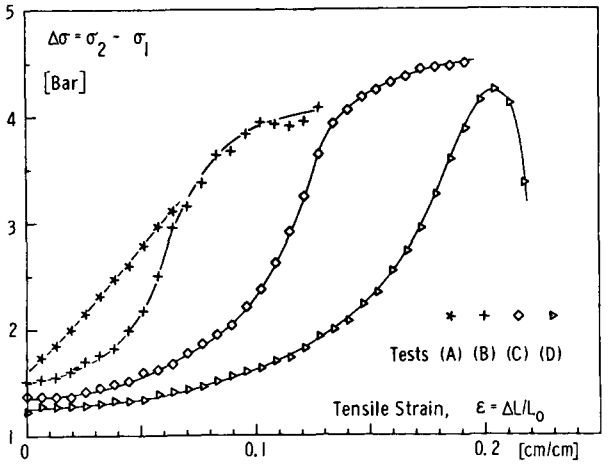

Fig. 5. Dynamic stresses during tests A to D.

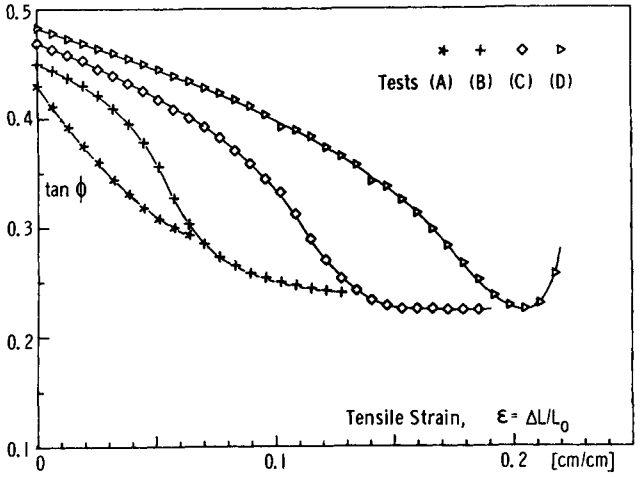

Fig. 6. Loss tangents during low straining with superposed tension oscillations.

A to test D, indicating a damage effect. The envelope for all four tests indicates the behavior of an initially undamaged sample from zero strain to failure. Dynamic energy losses per cycle are shown in Figure 7. The values are obtained from the single hysteresis recordings made every minute during the test. The curves for losses per cycle show the effect of increasing damage on the energy balance after each dewetting experiment. If a propellant is damaged within a certain strain region, the energy loss per cycle is found to be decreased during the second run below the same strain level. This damage does not increase during additional runs below the limits of the previous strain. When the previous strain limit is exceeded, the damage continues to increase again.

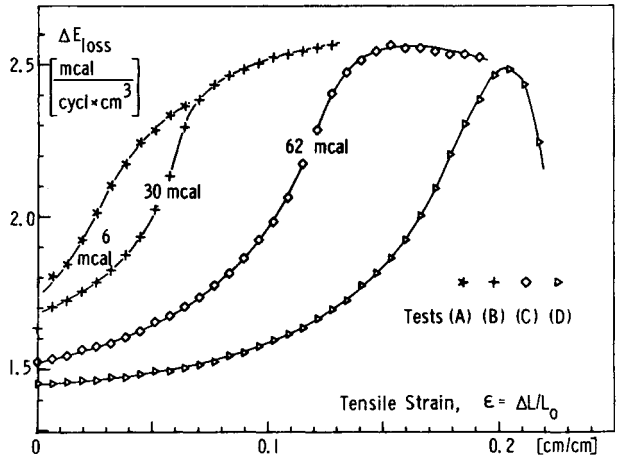

Fig. 7. Dynamic energy losses per cycle during tests A to D.

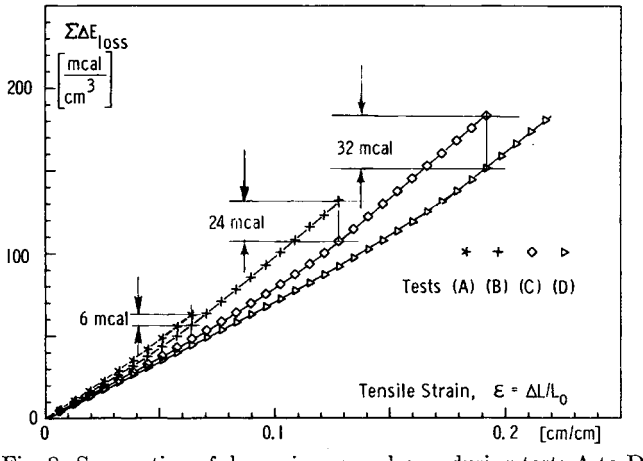

Fig. 8. Summation of dynamic energy losses during tests A to D.

The summation of the single hysteresis areas by eq. (5) are shown in Figure 8. The slope of the curve for the sum of the dynamic energy loss per cycle is a very sensitive indicator of the microstructural damage. By appropriately adding these microstructural energy losses, the total dynamic energy of an initially undamaged propellant from 0% strain to failure can be computed. The total energy loss at failure was found to be a characteristic propellant value and independent of the deformation path.

Fractional energy losses f_E and fractional energy losses per unit strain, f_E/ϵ, were determined from eq. (6). The results are plotted in Figures 9 and 10 and reveal a nonlinear damage behavior (with respect to strain) of the tested propellant between zero and 20% strain. The values f_E and f_E/ϵ in Figures 9 and 10 obtained from total input energy and loss energy

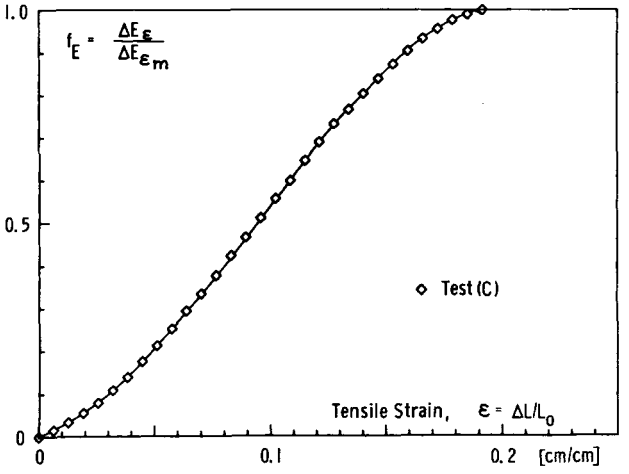

Fig. 9. Fractional energy losses per cycle vs. strain, test C.

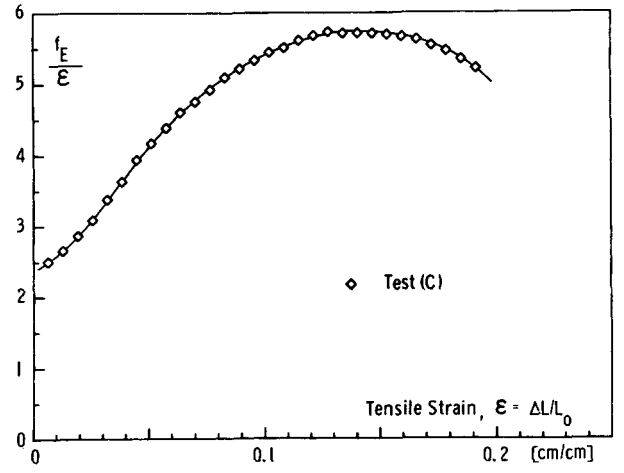

Fig. 10. Fractional cycling energy losses per cycle and per unit strain, test C.

balances per cycle have been found to be identical. Figures 9 and 10 are therefore satisfactory for both energy balances $\Sigma\Delta E_t$ and $\Sigma\Delta E_l$.

DISCUSSION OF RESULTS

Linear cumulative damage theory has been one of the most useful tools in the analysis of the mechanical performance of rocket motors and other plastic materials under a variety of temperatures and mechanical load cycling conditions. The cumulative damage criterion is based upon the assumption that exposure to stress above a certain low minimum stress induces a microscopic failure in the material. The longer the sample experiences the stress, the more extensive the damage as seen from eq. (1).

In the experiments reported in this paper, it is seen that it is the extent of strain rather than time at stress which dictates how the stress–strain curve will change. This is confirmed by the superposed oscillation studies. Further, at low strain values and at very high strain values in a low constant-strain rate experiment, the stress rate is nearly constant. It would be expected, then, that Figure 9 would show varying values for f_E/ϵ. This appears to be the case at intermediate strain values. It is suggested, therefore, that the linear cumulative damage theory is useful only because of the behavior of the f_E/ϵ curve (Fig. 9) at the intermediate strain values. This discussion does not suggest that the criterion be vitiated, but it does point out that a better criterion for propellants and highly filled materials might be strongly nonlinear. In addition, it may be more applicable for propellants if it can be formulated in terms of strain rather than stress.

It is of interest to observe (see Figs. 9 and 10) the accumulation of damage as a function of strain and the amount of damage that occurs in each increment of strain. The ordinate f_E in Figure 9 relates the damage to the maximum damage that can be experienced by a filled material, i.e., to failure. It should be noted that we consider here primarily failure in the viscoelastic transition region and not failure in the glassy region where the failure phenomenon is quite different. It is the experience in this laboratory that the dissipated failure energy is a constant for any one propellant. If this is so, then one can measure the energy required to fail a given propellant (or filled material) that has been studied in a fresh condition. One can then determine the extent or fraction of the useful life that has been lost by that particular sample in any subsequent state or condition. It is expected that this could, in time, lead to a strain-dependent formulation of a failure criterion. This corresponds to the intuitive way in which propellant chemists have tended to treat propellant properties over the years that the strain a sample can tolerate is more important than the failure stresses. Figure 10 can form the basis for such a formulation since it describes the fractional failure during each increment of strain.

CONCLUSIONS

The results of this investigation suggest that the dynamic test methods utilized in this paper are sensitive indicators of the damage occurring in highly filled systems. This damage appears to occur during the first stretch and does not sensibly increase upon repeated cycling below that first level of strain. The damage incurred by this process is not readily healed by allowing the sample to rest unstrained for as long as 50 hr at room temperature. This indicates that various kinds of permanent damage have occurred. Calculations strongly suggest that the major contribution of this energy loss is the rupture of primary chemical bonds. Dewetting energy losses play a secondary role. It was observed that the energy required to fail a propellant was independent of the mechanical path used to arrive at the failure. This fact suggests that, from reference curves for a partic-

ular material, it is possible to determine the fraction of the useful life lost by that material during an environmental history. It also appears that the primary damage criterion is more a strain-dependent criterion than a stress criterion. From the determination of damage occurring in the filled system per unit strain, it appears that the damage accumulates more in a nonlinear fashion than suggested by the usual linear cumulative damage criterion.

Appendix

Approximate Computation of Energies for Primary Bond Rupture and Adhesive Failure in a Propellant

PRIMARY BOND RUPTURE

A rough approximation to the rupture energy can be based on Bueche's expression[8] for the relationship between stress and strain involving the number of bonds supporting the load. Thus, we have

$$\sigma = \nu_e kT(\alpha - \alpha^2) \tag{7}$$

$$\nu_e = \nu(1 - 2M_c/M_n) \tag{8}$$

where T = absolute temperature, k = Boltzmann constant, θ = stress, ν = number of chains per unit volume, ν_e = number of effective chains, α = extension ratio, M_c = molecular weight of a network chain, and M_n = number-average molecular weight.

We note that the tensile strength at low crosslink densities varies almost linearly with the crosslink density. To obtain a conservative measure of the rupture energy, we assume that it is necessary to break crosslinked chains to develop failures. This is not unreasonable since, in the absence of the crosslinks, failure would not occur by a rupture process but by a flow process. For the purposes of this calculation, it is adequate to assume that rupture will occur when all crosslink chains are broken. Therefore, the energy required to break these crosslinks is a conservative estimate of the energy of failure resulting from primary bond rupture. In actual fact, many more carbon bonds will be ruptured during the process because of high local stress concentrations. Again, for this computation it is assumed that the rupture is a carbon–carbon rupture which requires about 82 kcal/mole of bonds. Rupture of a weaker bond such as an ester link would require about one fourth that amount of energy.

The crosslink densities for propellants have been determined in this laboratory to be of the order of 10^{-4} moles/cm^3. The rupture energy E_r for this process would then be

$$E_r = M_c \times 80 \text{ kcal/mole} \sim 8 \text{ cal/cm}^3.$$

ADHESIVE FAILURE

An order-of-magnitude estimate can be obtained by calculating the total energy attributable to dewetting per unit volume of propellant, E_{dw}. We write

$$E_{dw} = W_a A \tag{9}$$

where W_a is measured work of adhesion and A is the interfacial area per cm^3 of propellant. The latter is computed from the distribution of particle sizes, their weight fraction, and the densities of all components for an average propellant. With 80 erg/cm^2 for W_a, 3000 cm^2/cm^3 for A, and the common factor 2.39×10^{-8} cal/erg (reported by A. Adicoff, Pacific Conference in Chemistry and Spectroscopy, Anaheim California, October 31, 1967), we obtain E_{dw} as 5.73, $\times 10^{-3}$ cal/cm^3.

References

1. K. W. Bills, et al., *Final Report, Solid Propellant Cumulative Damage Program.* Aerojet-General Corporation, Propulsion Division, Sacramento, California, AFRPL-TR-68-131, October 1968.

2. R. J. Farris and L. R. Hermann, *Applications of Non-Linear Viscoelasticity and Cumulative Damage,* Aerojet Solid Propulsion Company, Sacramento, California, #1565-26F, May 1971.

3. G. H. Lindsey and J. E. Wood, *An Isotropic Theory of Dewettable Solids,* United States Naval Postgraduate School, Monterey, California, NPS-57Li71011A, January 31, 1971.

4. D. Saylack, et al., An Integrated Approach to Solid Propellant Cumulative Damage, *SRSI Abstracts,* Vol. 6, No. 3, 1969.

5. N. W. Tschoegl, W. G. Knauss, and R. F. Landel, *A Research Program on Solid Propellant Physical Behavior,* California Institute of Technology, AFRPL-TR-69-180, August 1969.

6. A. H. Lepie and A. Adicoff, *Rev. Sci. Instr.*, **38**, 1615 (1967).

7. A. H. Lepie, *Rev. Sci. Instr.*, **40**, 1004 (1969).

8. F. Bueche, *Physical Properties of Polymers,* Interscience, New York, 1962.

Received January 9, 1973